Design of Bimodal PCFs for Interferometric Gas Sensors With High Sensitivity

Teresa Pinheiro-Ortega, Enrique Silvestre, Pedro Andrés, Bjorn Maes, and Peter Bienstman, *Member, IEEE*

***Abstract*—We theoretically investigate bimodal photonic crystal fibers (PCFs) for the development of interferometric gas sensors (with one mode acting as the reference arm and another as the sensing arm), working either in the intensity measurement mode or in the spectral regime. For each operation mode we define a merit function that characterizes the sensitivity of the fiber taking into account both the interferometric and the evanescent-field nature of these sensing devices. The evaluation of the above merit functions, which involve the calculation of the propagation constant, the group index, and the field profile of the first two guided modes, allows us to identify highly sensitive microstructured fibers for each sensing mode. In this paper, we propose a single birefringent PCF design that exhibits in both regimes extreme sensitivity in a certain wavelength operation range that can be shifted by changing the air-filling fraction.**

***Index Terms*—Fiber design and fabrication, fiber optics sensors, photonic crystal fibers.**

I. INTRODUCTION

PHOTONIC CRYSTAL FIBERS (PCFs), also known as microstructured fibers, are characterized by the nearly periodic transverse distribution of air holes that run along the entire length of the fiber, which provides their unique guiding properties [1]. The microstructured cladding also permits an intimate interaction between the guided light that partially extends into the holes and a fluid diffused inside them, opening up new possibilities for evanescent field sensing [2]. The control of the geometrical parameters of these microstructured fibers permits a tailoring of their modal properties and, thus, designing in a flexible manner PCFs for sensor devices [3].

In the last years, intense work has been carried out in the development of PCF-based evanescent-wave sensors that characterize the gas or liquid located in the holey region through the transmission spectrum of the device, which is directly related to the spectral absorbance of the chemical species existing in the sample [4], [5]. Different designs have been proposed to enhance the sensitivity of these sensing devices by magnifying the overlap between the light and the fluid at issue [6]–[8].

The use of PCFs is also well known for the implementation of fiber-based interferometers. On one hand, to achieve the bimodal working operation regime, single-mode PCFs are combined with other fiber-based components as long-period fiber gratings [9] or solid taper waists [10], [11]. The above configurations have already been applied for gas and chemical sensing. On the other hand, it is possible to design fiber-based interferometers with bimodal PCFs, as well. They exhibit diverse geometries, highly birefringent patterns to maintain the polarization properties of the guided modes [12], [13] or regular short-length PCFs together with fusion splices [14]. The last designs have been successfully used for strain sensing. In this paper we examine bimodal PCFs for interferometric gas sensing. The first-order or fundamental mode, which is strongly confined in the solid core of the fiber, behaves as the reference arm of the interferometer and the second-order mode, which partially spreads over the holey region, plays the role of the sensing arm.

The above fiber-based interferometers commonly operate with two detection approaches: the "intensity measurement mode," where the output intensity is detected as a function of the parameter to be determined [11], [12], and a potentially more robust one, the "spectral mode," where the frequency minima of the output intensity are correlated with the magnitude under study [10], [14]. It is convenient that these bimodal devices operate with the same design in a broad wavelength range in order to increase their sensing possibilities. In this respect, PCFs are excellent candidates since they can exhibit an extremely wide spectral range for bimodal operation [15]. In the design process of our bimodal PCFs, we consider both operation modes. Accordingly, we define for each one a merit function that characterizes the sensitivity of the procedure taking into account both the interferometric and the evanescent-field nature of these sensing devices. We focus our attention on the design of birefringent PCFs with a broadband bimodal operation regime and an extremely high sensitivity to small variations of the refractive index of the sample to be measured.

II. MATHEMATICAL FORMULATION: DEFINITION OF MERIT FUNCTIONS

As is well known, the interference pattern of a Mach–Zehnder interferometer is regulated by the phase shift between the light traveling along its two arms, which in the case of a bimodal PCF corresponds to $\Delta\theta = (\beta_2 - \beta_1)l$, where β_i $(i = 1, 2)$ stands for

Manuscript received August 26, 2009; revised December 29, 2009; accepted February 21, 2010. Date of current version May 19, 2010. This work was supported in part by the Ministerio de Ciencia e Innovación, Spain, under Grant TEC2008-05490 and by the Generalitat Valenciana under Grant PROMETEO2009/077, and by COST Action MP0702. The work of T. Pinheiro-Ortega was supported in part by MEC, Spain, under an FPU grant. The work of B. Maes was supported in part by the Research Foundation-Flanders. The associate editor coordinating the review of this paper and approving it for publication was Dr. Cristiano Cordeiro.

T. Pinheiro-Ortega, E. Silvestre, and P. Andrés are with the Department of Optics, Universitat de València, 46100 Burjassot, Spain (e-mail: teresa.pinheiro@uv.es).

B. Maes and P. Bienstman are with the Photonics Research Group, Department of Information Technology, Ghent University-IMEC, 9000 Ghent, Belgium.

Color versions of one or more of the figures in this paper are available online at http://ieeexplore.ieee.org.

Digital Object Identifier 10.1109/JSEN.2010.2046032

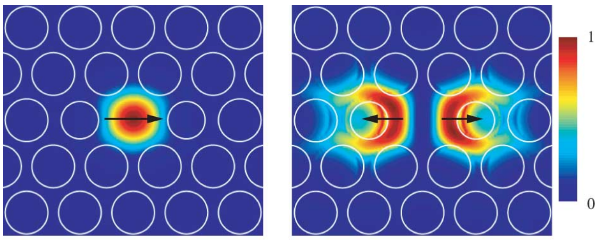

Fig. 1. Intensity field profile for a birefringent PCF: (a) fundamental mode and (b) second-order guided mode with vertical nodal line. The arrows represent the electric field polarization state corresponding to each mode.

the propagation constant of the fundamental and second-order guided mode, respectively, and l is the fiber length. From the beginning it is important to point out that the interference pattern is affected by any change of the refractive index of the sample, n_s, diffused in the holes of the fiber because the evanescent field overlapping within the holey region is different for each guided mode (see Fig. 1).

First, we consider the intensity sensing approach. It is based on the detection of the output intensity, $I = I_0(1 + V\cos\Delta\theta)$, at a fixed wavelength, λ_0, as a function of n_s. V is the visibility of the interference pattern. In mathematical terms, the variation of I with n_s is given by

$$\frac{dI}{dn_s} \propto \sin\Delta\theta \frac{d\Delta\theta}{dn_s} \tag{1}$$

where $\Delta\theta$ depends on n_s through β_i. As it is recognized in [16], the first derivative of β_i with respect to n_s, β_i', can be computed through the closed expression $\beta_i' = \langle L'\rangle_i/2\beta_i$, where the prime indicates differentiation with respect to n_s and $\langle L'\rangle_i = \langle\tilde{h}_{t(i)}|L'h_{t(i)}\rangle/\langle\tilde{h}_{t(i)}|h_{t(i)}\rangle$ represents the expectation value of the operator L' for the pair of dual fields of the ith mode. L is the differential operator of the 2-D wave equation for the transverse components of the magnetic field, h_t, and $\tilde{h}_t$ denotes the dual field of h_t. The integral formulation of the above expectation value is given by

$$\langle L'\rangle_i = \frac{\int \tilde{h}_{t(i)} L' h_{t(i)} dx dy}{\int \tilde{h}_{t(i)} h_{t(i)} dx dy}. \tag{2}$$

At this point we realize that it is convenient to define the merit function of this operation mode as

$$M_I = n'_{\text{eff}(2)} - n'_{\text{eff}(1)} \tag{3}$$

being $n_{\text{eff}(i)}$ $(i = 1, 2)$ the effective index of the corresponding mode. Using the above expressions for the derivatives, the sensitivity function can be evaluated as

$$M_I = \frac{1}{2(\omega_0/c)}\left(\frac{\langle L'\rangle_2}{\beta_2} - \frac{\langle L'\rangle_1}{\beta_1}\right) \tag{4}$$

where the vector nature of the electromagnetic propagation is still preserved. In order to gain some physical insight in the above merit function, as a first approach, we disregard the vector terms of L for reducing the mathematical complexity in (4). So, within a first-order approximation, we consider $L = \nabla_t^2 + [(\omega/c)n(x_t)]^2$, and accordingly $\langle L'\rangle_i = 2(\omega/c)^2 n_s f_i$, being $f_i = \langle\tilde{h}_{t(i)}|h_{t(i)}\rangle_A/\langle\tilde{h}_{t(i)}|h_{t(i)}\rangle$ the fraction of total power inside the holes (region A) for the ith guided mode. By using the relative sensitivity coefficient outlined by Hoo *et al.* [4], $r_i = (n_s/n_{\text{eff}(i)})f_i$, the merit function becomes

$$M_I = r_2 - r_1. \tag{5}$$

As a matter of fact, the output intensity can be affected by several unwanted factors (source intensity fluctuations, device aging, etc.), resulting in a gradual loss of accuracy. A more robust alternative is the spectral sensing approach. Now we assume polychromatic light and focus our attention on the case of destructive interference. The mth minimum of the spectral content of I, say ω_m, is determined by the expression

$$\begin{aligned}\Delta\theta &= \{\beta_2[\omega_m(n_s), n_s] - \beta_1[\omega_m(n_s), n_s]\}l \\ &= (2m+1)\pi\end{aligned} \tag{6}$$

where m is an integer. We define the new merit function as $M_\omega = \omega_m'/\omega_m$. If we perform the total derivative with respect to n_s in (6), we obtain

$$\dot{\beta}_2\omega_m' + \beta_2' - \dot{\beta}_1\omega_m' - \beta_1' = 0 \tag{7}$$

and operating

$$M_\omega = \frac{\beta_2' - \beta_1'}{\omega_m(\dot{\beta}_1 - \dot{\beta}_2)} \tag{8}$$

where the overdot indicates differentiation with respect to ω_m. As in the intensity operation mode, the latter sensitivity function can be also rewritten in terms of expectation values as

$$M_\omega = \frac{1}{\omega_m}\left(\frac{\langle L'\rangle_2}{\beta_2} - \frac{\langle L'\rangle_1}{\beta_1}\right)\left(\frac{\langle \dot{L}\rangle_2}{\beta_2} - \frac{\langle \dot{L}\rangle_1}{\beta_1}\right)^{-1}. \tag{9}$$

Again in the framework of a first-order approximation, (9) can be written as

$$M_\omega = (r_2 - r_1)(n_{g(1)} - n_{g(2)})^{-1} \tag{10}$$

where $n_{g(i)}$ $(i = 1, 2)$ stands for the group index of the corresponding guided mode.

Note that each operation mode is characterized by a different dimensionless sensitivity function. However, in both cases the factor $\Delta r = r_2 - r_1$ appears, and consequently must be maximized. This fact entails the enhancement of the evanescent field inside the air holes for the second-order mode and the corresponding minimization for the fundamental one. It is also very important to recognize that the function M_ω involves the factor $(n_{g(1)} - n_{g(2)})^{-1}$. Therefore, the sensitivity of the spectral approach is higher and higher as the group birefringence between the two considered modes is lower and lower.

III. Design Procedure

In this section we apply the mathematical formulation previously developed to design a highly sensitive bimodal PCF for interferometric gas sensing. Although several PCF geometries can achieve high values for the proposed merit functions, in this

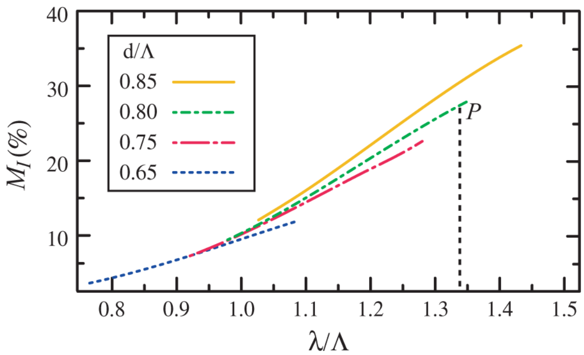

Fig. 2. Merit function M_I as a function of λ/Λ for different values of d/Λ corresponding to the geometry of the birefringent PCF shown in Fig. 1.

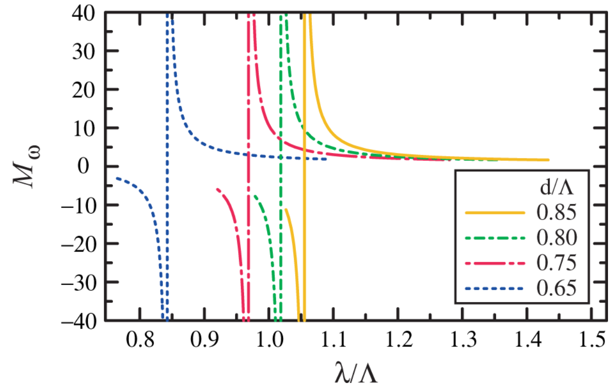

Fig. 3. The same as in Fig. 2, but for the merit function M_ω.

paper we are interested in the identification of at least one structure that shows high sensitivity for the intensity measurement mode and the spectral regime, simultaneously.

Bearing in mind the interferometric nature of the device, it is suitable to select a birefringent geometry for the fiber. This choice breaks down the near degeneration of the guided modes and consequently assures the absence of intermodal beating. In this way, selecting the proper illumination strategy, it is feasible to make interfere only two nondegenerated modes with the same linear polarization state, one from the fundamental doublet and another from the four modes that constitute the second-order multiplet. We propose the structure shown in Fig. 1, where the birefringence is introduced by means of two smaller holes in the first ring. This selection permits us to obtain a broader bimodal wavelength range. For the rest of this section we have fixed the relation between the diameter of the smaller holes, d_1, the pitch, Λ, and the diameter for the rest of holes, d, as $d - d_1 = \Lambda/10$.

In a first-order approximation, both merit functions, defined by (5) and (10), require the evaluation of the effective index and the transverse field profile for the first two guided modes to compute r_i, as well as the calculation of the group birefringence for the spectral operation mode. To do so, we use the 2-D iterative Fourier modal method described in [17] and assume $n_s = 1$ as a good approximation for the standard value of the refractive index of most gases. Taking into account the scale invariance satisfied by the two dimensionless merit functions due to the scaling properties of the Maxwell equations, our design parameters are, in fact, the relative hole diameter, d/Λ, which is directly related with the air-filling fraction, and the normalized wavelength, λ/Λ.

In relation to the intensity measurement procedure, in Fig. 2 we represent M_I as a function of λ/Λ for several values of d/Λ. Each curve ranges over the wavelength interval in which the PCF is bimodal. As was expected, the sensitivity of the fiber increases with the design parameter d/Λ. According to Fig. 2, once λ_0 is fixed by the laser source, we must choose the values of Λ and d/Λ in order to reach both the bimodal region and a high sensitive fiber geometry. For example, if $\lambda_0 = 1.55$ μm, we select $\Lambda = 1.15$ μm ($\lambda/\Lambda = 1.348$) and $d = 0.92$ μm ($d/\Lambda = 0.8$), which corresponds to the point P in Fig. 2. In fact, it is precisely this fiber which is represented in Fig. 1 and the current design involves a value of $\Delta r = r_2 - r_1$ of around 27%.

Next, we evaluate the merit function for the spectral sensing approach. As before, for the birefringent geometry sketched in Fig. 1 we vary the design parameters d/Λ and λ/Λ within the bimodal range. In this way, in Fig. 3 we represent M_ω as a function of λ/Λ for the same discrete values of the parameter d/Λ as in Fig. 2.

In this approach, we recognize that M_ω has a divergence at a certain normalized wavelength, $(\lambda/\Lambda)_D$, due to the cancellation of the term $(n_{g(1)} - n_{g(2)})^{-1}$. For this particular spectral point, the intermodal group birefringence is zero and the interference term is minimum simultaneously. Therefore this is a highly sensitive point, where any change in the refractive index of the sample will produce a great variation in the intensity minimum. Up to now we have developed a first-order theory for the evaluation of the function M_ω. It is important to point out that if we consider a second-order perturbation theory for the mathematical formulation of M_ω, the divergence will become into a high but finite value, which will be located at the same wavelength. So, if we are working near this critical point we approximate, similarly to [18]

$$\left(n_{g(1)} - n_{g(2)}\right)(\lambda) \approx \left(n_{g(1)} - n_{g(2)}\right)|_{\lambda_D} + \Delta\lambda \frac{d}{d\lambda}\left(n_{g(1)} - n_{g(2)}\right)\Big|_{\lambda_D} \qquad (11)$$

in order to obtain a finite value for the sensitivity, where $\Delta\lambda$ should be taken as the device's nominal wavelength discrimination. As an example, if we consider the geometric parameters $\Lambda = 1.85$ μm and $d = 1.388$ μm, which correspond to $d/\Lambda = 0.75$, the normalized divergence wavelength has been found in $(\lambda/\Lambda)_D = 0.969$. If we consider in the previous approach a typical nominal wavelength resolution of $\Delta\lambda = 0.0025$ nm, as in [19], the merit function reaches the value $M_\omega \approx 2.3 \times 10^5$ in the critical point, which corresponds to a theoretical resolution in the refractive index of the sample of $\Delta n_s = 6.0 \times 10^{-12}$ RIU. Of course, in this evaluation we have not considered the thermooptic effect in silica. We could also evaluate an effective wavelength resolution from the theoretical spectral interferogram calculated for a concrete length of the device. As an example, for the above case and considering a fiber length $l = 1$ cm, we have estimated $\Delta\lambda = 13$ nm as the tenth of the fringe width defined as the spectral separation between the two minima located in the vicinity of the critical point. This wavelength resolution would provide a value of $M_\omega \approx 8 \times 10^4$ in the critical point and, correspondingly, a more realistic value of $\Delta n_s = 1.6 \times 10^{-4}$ RIU. Similar calculations could be done for the rest of curves in Fig. 3 with a different d/Λ value.

If we compare Figs. 2 and 3, we note that the region where the values of the sensitivity function are greater in each plot is shifted. In this way, next we consider in the spectral regime a similar example as the one previously presented for the intensity measurement mode, i.e., the intensity minimum for $\lambda = 1.55\ \mu$m and $d/\Lambda = 0.8$. For this particular case, the normalized divergence wavelength turns out $(\lambda/\Lambda)_D = 1.018$, which is in agreement with Fig. 3, and in the framework of a first-order perturbation theory, the fiber parameters are now $\Lambda = 1.52\ \mu$m and $d = 1.22\ \mu$m.

Further studies concerning confinement losses should be carried out in order to appropriately characterize the potentiality of the current fiber for gas sensing purposes. However, as a first approach, the estimated confinement of the guided modes would suggest a reasonable behavior of the system if a short length is considered, which is highly recommended for gas diffusion inside the holes of the fiber. It is apparent that the problem of gas infiltration in the microholes is out of the scope of this paper. Other technological questions should be also considered in the design of the entire sensing device, such as splice losses between the PCF sensor and other input/output fibers, which could be significantly reduced by using the microhole collapse property [20] or other appropriate techniques.

IV. Conclusion

In this paper, we have theoretically considered the implementation of interferometric gas sensors based on bimodal PCFs. We have presented some merit functions that characterize the sensitivity of the fiber for two common operation manners, the intensity and the spectral measurement regimes. These functions take into consideration both the interferometric and the evanescent-field nature of these sensing devices and should be maximized to enhance the sensitivity of the method. Their evaluation just implies the calculation of the propagation constant, the group index, and the field profile of the guided modes. We have also proposed the design of a birefringent PCF with two smaller inner holes in the first ring to accomplish the above goals. This geometry results on the increase of the bimodal spectral range of the fiber, that is, its spectral working regime. For the suggested design, the above two merit functions have been analyzed for different air-filling fractions. They certainly exhibit extremely high values, so that the previous PCF could be regarded as a good candidate for the development of gas sensing devices.

References

[1] P. St and J. Russell, "Photonic-crystal fibers," *J. Lightwave Technol.*, vol. 24, pp. 4729–4749, 2006.

[2] T. M. Monro, D. J. Richardson, and P. J. Bennett, "Developing holey fibres for evanescent field devices," *Electron. Lett.*, vol. 35, pp. 1188–1189, 1999.

[3] T. M. Monro, W. Belardi, K. Furusawa, J. C. Baggett, N. G. R. Broderick, and D. J. Richardson, "Sensing with microstructured optical fibres," *Meas. Sci. Technol.*, vol. 12, pp. 854–858, 2001.

[4] Y. L. Hoo, W. Jin, C. Z. Shi, H. L. Ho, D. N. Wang, and S. C. Ruan, "Design and modeling of a photonic crystal fiber gas sensor," *Appl. Opt.*, vol. 42, pp. 3509–3515, 2003.

[5] J. B. Jensen, L. H. Pedersen, P. E. Hoiby, L. B. Nielsen, T. P. Hansen, J. R. Folkenberg, J. Riishede, D. Noordegraaf, K. Nielsen, A. Carlsen, and A. Bjarklev, "Photonic crystal fiber based evanescent-wave sensor for detection of biomolecules in aqueous solutions," *Opt. Lett.*, vol. 29, pp. 1974–1976, 2004.

[6] T. Ritari, J. Tuominen, H. Ludvigsen, J. C. Petersen, T. Sorensen, T. P. Hansen, and H. R. Simonsen, "Gas sensing using air-guiding photonic bandgap fibers," *Opt. Expr.*, vol. 12, pp. 4080–4087, 2004.

[7] J. M. Fini, "Microstructure fibres for optical sensing in gases and liquids," *Meas. Sci. Technol.*, vol. 15, pp. 1120–1128, 2004.

[8] C. M. B. Cordeiro, M. A. R. Franco, G. Chesini, E. C. S. Barretto, R. Lwin, C. H. B. Cruz, and M. C. J. Large, "Microstructured-core optical fibre for evanescent sensing applications," *Opt. Expr.*, vol. 14, pp. 13056–13066, 2006.

[9] J. H. Lim, H. S. Jang, K. S. Lee, J. C. Kim, and B. H. Lee, "Mach-Zehnder interferometer formed in a photonic crystal fiber based on a pair of long-period fiber gratings," *Opt. Lett.*, vol. 29, pp. 346–348, 2004.

[10] V. P. Minkovich, J. Villatoro, D. Monzón-Hernández, S. Calixto, A. B. Sotsky, and L. I. Sotskaya, "Holey fiber tapers with resonance transmission for high-resolution refractive index sensing," *Opt. Expr.*, vol. 13, pp. 7609–7614, 2005.

[11] V. P. Minkovich, D. Monzón-Hernández, J. Villatoro, and G. Badenes, "Microstructured optical fiber coated with thin films for gas and chemical sensing," *Opt. Expr.*, vol. 14, pp. 8413–8418, 2006.

[12] J. Ju, W. Jin, and M. S. Demokan, "Two-mode operation in highly birefringent photonic crystal fiber," *IEEE Photon. Technol. Lett.*, vol. 16, pp. 2472–2474, Nov. 2004.

[13] Z. Wang, J. Ju, and W. Jin, "Optimizing PCFs for two-mode interference," *Opt. Fiber Technol.*, vol. 12, pp. 29–37, 2006.

[14] J. Villatoro, V. P. Minkovich, V. Pruneri, and G. Badenes, "Simple all-microstructured-optical-fiber interferometer built via fusion splicing," *Opt. Expr.*, vol. 15, pp. 1491–1496, 2007.

[15] W. Jin, Z. Wang, and J. Ju, "Two-mode photonic crystal fibers," *Opt. Expr.*, vol. 13, pp. 2082–2088, 2005.

[16] E. Silvestre, T. Pinheiro-Ortega, P. Andrés, J. J. Miret, and A. Coves, "Differential toolbox to shape dispersion behavior in photonic crystal fibers," *Opt. Lett.*, vol. 31, pp. 1190–1192, 2006.

[17] E. Silvestre, T. Pinheiro-Ortega, P. Andrés, J. J. Miret, and A. Ortigosa-Blanch, "Analytical evaluation of chromatic dispersion in photonic crystal fibers," *Opt. Lett.*, vol. 30, pp. 453–455, 2005.

[18] R. Levy and S. Ruschin, "Critical sensitivity in hetero-modal interferometric sensor using spectral interrogation," *Opt. Expr.*, vol. 16, pp. 20516–20521, 2008.

[19] J. Dostalek, J. Ctyroky, J. Homola, E. Brynda, M. Skalsky, P. Nekvindova, J. Spirkova, J. Skvor, and J. Schrofel, "Surface plasmon resonance biosensor based on integrated optical waveguide," *Sens. Actuators B*, vol. 76, pp. 8–12, 2001.

[20] L. Xiao, M. S. Demokan, W. Jin, Y. Wang, and C. Zhao, "Fusion splicing photonic crystal fibers and conventional single-mode fibers: Microhole collapse effect," *J. Lightwave Technol.*, vol. 25, pp. 3563–3574, 2007.

Teresa Pinheiro-Ortega was born in Alicante, Spain, in 1980. She received the Dipl. degree in physics and the Ph.D. degree in physics/optics from the University of Valencia, Valencia, Spain, in 2003 and 2008, respectively.

Since 2008, she has been with the R&D Department, Aurora Software and Testing Company, where her research concerns the electromagnetic analysis and design of microwave passive components in terms of power handling.

Pedro Andrés was born in Valencia, Spain, in 1954. He received the Ph.D. degree in physics/optics from the University of Valencia, Valencia, Spain, in 1983.

He has been a Full Professor of Optics with the University of Valencia since 1994. He acted as Head of the Department of Optics, University of Valencia, from 1998 to 2006. He has coauthored more than 100 peer-reviewed papers, some of them in collaboration with European and/or American researchers, and has presented 29 invited papers at international conferences and meetings. His current research interests include diffractive optics, confocal scanning microscopy, modeling and design of photonic crystal fibers, temporal optics, and ultrafast optics.

Dr. Andrés is a Fellow of the Optical Society of America and a member of the European Optical Society Board of Directors.

Bjorn Maes (M'09) received the Engineering degree in applied physics in 2001 from Ghent University, Ghent, Belgium, and the Ph.D. degree from the Photonics Research Group, Ghent University, in 2005.

During 2005–2006, he was a Postdoctoral Associate with the Joannopoulos Research Group, Massachusetts Institute of Technology (MIT). Currently he is a FWO Postdoctoral Fellow with the Photonics Research Group, Ghent University. His research interests include the numerical and theoretical modeling of nanophotonic devices and integrated circuits. More specifically, he is working on the physics of photonic crystals, plasmonics, nonlinear photonics, and solar cells.

Peter Bienstman was born in Ghent, Belgium, in 1974. He received the Degree in electrical engineering and the Ph.D. degree from Ghent University, Ghent, Belgium, in 1997 and 2001, respectively.

He is currently an Associate Professor with the Department of Information Technology (INTEC), Ghent University. During 2001–2002, he was with the Joannopoulos Research Group, Massachusetts Institute of Technology (MIT). He has published over 50 papers and holds several patents. His research interests include several applications of nanophotonics (biosensors and photonic information processing), as well as nanophotonics modeling.

Dr. Bienstman is a member of the IEEE Lasers and Electro-Optics Society.